

Upper limit to magnetism in LaAlO₃/SrTiO₃ heterostructures

M. R. Fitzsimmons,¹ N. Hengartner,¹ S. Singh,^{1,2} M. Zhernenkov,¹ F. Y. Bruno³, J. Santamaria,³ A. Brinkman,⁴ M. Huijben,⁴ H. Molegraaf,⁴ J. de la Venta,⁵ and Ivan K. Schuller⁵

¹Los Alamos National Laboratory, Los Alamos NM 87545 USA

²Solid State Physics Division, Bhabha Atomic Research center, Mumbai- 400085, India

³GFMC. Dpto. Fisica Aplicada III, Universidad Complutense de Madrid, 28040 Madrid. Spain

⁴MESA+ Institute for Nanotechnology, University of Twente, Enschede, The Netherlands

⁵Department of Physics and Center for Advanced Nanoscience, University of California San Diego, La Jolla, CA 92093 USA

Abstract—Using polarized neutron reflectometry (PNR) we measured the neutron spin dependent reflectivity from four LaAlO₃/SrTiO₃ superlattices. This experiment implies that the upper limit for the magnetization induced by an 11 T magnetic field at 1.7 K is 2 emu/cm³. SQUID magnetometry of the superlattices sporadically finds an enhanced moment, possibly due to experimental artifacts. These observations set important restrictions on theories which imply a strongly enhanced magnetism at the interface between LaAlO₃ and SrTiO₃.

PACS: 75.70.-i, 75.70.Cn, 61.05.fj

LAUR 11-04816

In 2004 Ohtomo and Hwang¹ reported that the interface between LaAlO₃ and SrTiO₃ films was conducting. Since 2004 there have been numerous reports of metallic conduction,^{1,2} superconductivity,^{3,4} magnetism,⁵ and coexistence of superconductivity and ferromagnetism⁶ that have been attributed to LaAlO₃/ SrTiO₃ interfaces. On the other hand, superconductivity of oxygen deficient SrTiO₃ has been established for decades.⁷ The conductivity in the LaAlO₃/ SrTiO₃ system may arise from intrinsic effects such as the polar catastrophe,^{8,9} or extrinsic defects such as oxygen vacancies^{10,11,12,13} or cation diffusion,^{14,15,16} and structural distortion/orbital reconstruction.¹⁷

The presence of magnetic local moments at the LaAlO₃/ SrTiO₃ interface was inferred from the magnetoresistance of a (high O partial pressure grown) LaAlO₃/ SrTiO₃ interface at low temperature in high magnetic fields.^{5,6,18} The location and magnitude of magnetic moments in LaAlO₃/ SrTiO₃ heterostructures remains unknown. Ferromagnetism (at room temperature), paramagnetism and diamagnetism (below 60 K) were claimed for 10 unit cells of LaAlO₃ on SrTiO₃ in a moderate field.¹⁹ Recent torque magnetometry measurements report moments as large as 4×10^{-10} Am² for 5 unit cells of LaAlO₃ on SrTiO₃.²⁰ When attributed to the entire LaAlO₃ film, the saturation magnetization claimed from these measurements range between 10 and 30 emu/cm³—a readily detectable signal with neutron scattering.²¹ If attributed to just one unit at the LaAlO₃ on SrTiO₃ interface,²⁰ the magnetization is noticeably larger. The large moments attributed to interfaces rely on measurement techniques that are unable to distinguish between interfacial and bulk magnetism. On the other hand, a number of experimental artifacts may produce spurious results due to extrinsic effects.^{22,23} Because of this, it is imperative to perform magnetic measurements which are impervious to many experimental

artifacts of which bulk measurements suffer, and to use techniques that are intrinsically sensitive to interface magnetism.

We have performed extensive polarized neutron reflectometry (PNR) measurements of $\text{LaAlO}_3/\text{SrTiO}_3$ superlattices. In spite of the fact that bulk measurements of our samples (and those of others^{19,20}) imply a magnetization as high as 60 emu/cm^3 if attributed to the superlattice, PNR unequivocally establishes an upper limit of 2 emu/cm^3 on their magnetization. It is important to note that the present measurements are done at fields as high as 11T and temperatures as low as 1.7K. The PNR results have serious implications for theories developed to explain magnetism in oxide superlattices.^{24,25,26}

$\text{LaAlO}_3/\text{SrTiO}_3$ superlattice samples were grown independently at laboratories located in Twente and Madrid. The Twente samples were grown on TiO_2 terminated SrTiO_3 single crystal substrates. $[(\text{LaAlO}_3)_8/(\text{SrTiO}_3)_{24}]_{30}$ (Twente1) and $[(\text{LaAlO}_3)_4/(\text{SrTiO}_3)_{12}]_{30}$ (Twente2) superlattices were fabricated by pulsed laser deposition with reflection high-energy electron diffraction (RHEED) control of the growth process. Single-crystal LaAlO_3 and SrTiO_3 targets were ablated at a laser fluence of 1.3 J/cm^2 and a repetition rate of 1 Hz. During growth, the substrate was held at $850 \text{ }^\circ\text{C}$ in an oxygen environment at $2 \times 10^{-3} \text{ mbar}$ for LaAlO_3 and SrTiO_3 . RHEED intensity oscillations were observed during growth of each individual layer indicating control on the unit cell scale due to the layer-by-layer growth mode. After growth, the superlattices were cooled to room temperature in $2 \times 10^{-3} \text{ mbar}$ of oxygen at a rate of $10 \text{ }^\circ\text{C/min}$. Atomic force microscopy (AFM) showed smooth terraces separated by unit cell high steps similar to the surface of the initial TiO_2 -terminated SrTiO_3 (100) substrate.

$[(\text{LaAlO}_3)_8/(\text{SrTiO}_3)_{24}]_{30}$ (Madrid2) and $[(\text{LaAlO}_3)_4/(\text{SrTiO}_3)_{12}]_{15}$ (Madrid1) were grown on TiO_2 terminated (001) STO substrates using high-pressure (2.9 mbar) pure oxygen sputtering at a substrate temperature of 750 °C. After growth the samples were cooled to 600 °C. At this temperature the chamber was filled with 900 mbar O_2 , and the samples were annealed for 5 minutes at 550 °C before completing the cooling to room temperature at a 20 °C/min rate.

The physical structure is determined from the wavevector transfer (Q)-dependence of the X-ray reflectivity which is sensitive to the uniformity of layer thicknesses and interface roughness averaged over lateral dimensions of several microns. The broadening of the superlattice reflections implies that the layer thicknesses varied across the sample (along its surface normal) by more than half a unit cell. Furthermore, the positions of the superlattice reflections for the Madrid1 and Twente2 samples were shifted slightly towards larger Q compared to the simulation implying the LaAlO_3 layer thicknesses for these samples may be (3.5 ± 0.5) unit cells thick rather than 4 unit cells as intended. On the other hand, the LaAlO_3 thickness of Samples Twente1 and Madrid2 were closer to the intended thickness of 8 unit cells.

To test whether our $\text{LaAlO}_3/\text{SrTiO}_3$ heterostructures are magnetic, we measured the depth dependence of magnetization for several $\text{LaAlO}_3/\text{SrTiO}_3$ superlattices at different fields and temperatures with polarized neutron reflectometry (PNR).^{27,28,29} In PNR the intensity of specularly reflected neutrons is compared to the intensity of the incident beam as a function of Q and neutron beam polarization. The specular reflectivity, R, is determined by the neutron scattering length density depth profile, $\rho(z)$, averaged over the lateral dimensions of the

sample. $\rho(z)$ consists of nuclear and magnetic scattering length densities such that

, where $C = 2.853 \times 10^{-9} \text{ \AA}^{-2} \text{ cm}^3 / \text{emu}$ and $M(z)$ is the depth profile of the magnetization (in emu/cm^3) parallel to the applied field.²⁹ The \pm sign denotes neutron beam polarization parallel (opposite) to the applied field. Thus, by measuring $R^+(Q)$ and $R^-(Q)$, and $\frac{R^+(Q) - R^-(Q)}{R^+(Q) + R^-(Q)}$ can be obtained separately. The difference between $R^+(Q)$ and $R^-(Q)$ or the difference divided by the sum, the “spin asymmetry”, is very sensitive to small M values. A major advantage of PNR is the ability to distinguish magnetism at an interface or a thin film, from the substrate. Measurements of the spin-dependent superlattice reflection assure that variations of M having the period of the superlattice and not spurious contamination from other sources are measured. Thus, we should stress that the important concerns raised regarding bulk magnetometry of materials with nanometer dimensions and phantom magnetism²³ are not germane to PNR.

Detection of small M can be problematical even for PNR. First, the difference between R^+ and R^- may be so small that the difference is not statistically significant. This difference can be substantially enhanced using a superlattice, where many interfaces contribute to the superlattice reflection. Additionally, a neutron scattering instrument may bias one spin state over the other. For example, to reverse the neutron beam polarization a neutron spin flipper is turned off or on, thus treating the two polarizations differently which may induce a systematic error on R^+ or R^- . Previously, we have shown the instrumental bias for the Asterix reflectometer/diffractometer is less than one part in 1000.³⁰

In order to further suppress instrumental bias, we developed a new measurement protocol for this experiment. Two samples measured at the same time were compared—a LaAlO₃/ SrTiO₃ superlattice, and a control sample (in this case a MgO single crystal substrate). The samples were mounted on a special holder with approximately 1° difference between their surface normals [Figures 1(a) and 1(b)]. Thus, the specularly reflected beams corresponding to the superlattice reflection from the LaAlO₃/ SrTiO₃ and the region of total reflection from the control sample appear in different locations of a position sensitive neutron detector [Figure 1(c)]. The neutron intensity was measured as a function of wavelength λ for fixed scattering angle 2θ from which we obtain —. The incident beam intensity for each spin state was determined using a portion of the spectrum of the neutron beam reflected by the control sample. This protocol normalizes out instrumental artifacts that might produce a false spin asymmetry, since the sample and control are measured simultaneously.

Samples and control were cooled in an 11 T field from room temperature to 1.7 K. The spin dependent reflectivities were simultaneously recorded as functions of field and temperature using the Asterix spectrometer at LANSCE. The data were corrected for variation of the neutron spectrum and wavelength dependent variation of the efficiencies of the neutron polarizer and spin flipper.³¹

Figure 2(a) shows the reflectivity of Sample Twente1 near its critical edge (where the sample's reflectivity is unity) and over a range of Q which includes the Bragg reflection for Sample Madrid1 (inset). The Q -dependent spin asymmetry near the critical edge near $Q_c = 0.0133 \text{ \AA}^{-1}$ for SrTiO₃, which is sensitive to the net magnetization, is shown for Sample Twente1

in Figure 2(b). These data were analyzed using the method of Parratt³² assuming a uniformly distributed magnetization depth profile. A magnetization (-0.12 ± 1.2) emu/cm³ was obtained implying a statistically insignificant spin asymmetry at the critical edge of the LaAlO₃/SrTiO₃. The influence on the spin asymmetry of magnetization equal to -0.12, 1, and 10 emu/cm³ uniformly distributed throughout the superlattice are shown by the red, dashed and blue curves in Figure 2(b), respectively.

To quantify influence of field and temperature on the spin dependence of the Bragg reflections from the LaAlO₃/SrTiO₃ [an example is shown in the inset of Figure 2(a)], we define a spin asymmetry ratio (SAR). This ratio is equal to the difference between the *integrated intensities* of the spin dependent superlattice reflections divided by their sum.³³ Figure 3 shows the SAR for Sample Twente1 as a function of field for two temperatures averaged from two separate experiments. Figure 4 shows the SAR for four samples measured at 11 T and 1.7 K.

The spin asymmetry of the superlattice reflection is sensitive to changes of magnetization having the period of the superlattice. It is possible for such changes to be too small to produce spin asymmetry at the critical edge. For example, the magnetization may change sign as a function of depth, or it may be confined to an interface, i.e., to a small fraction of the superlattice.

In Figure 3 we define the slope from the best fits to the data weighted according to the 1-sigma errors which gives a 1-sigma error on the slope. The slope of the 1.7 K data (closed symbols, Figure 3), $(-0.0006 \pm 0.0002) \text{ T}^{-1}$ is statistically different than zero and suggests that *the*

SAR becomes more negative as the field increases. On the other hand, the slope for the 80 K data (open symbols, Figure 3), $(-0.0003 \pm 0.0003) \text{ T}^{-1}$ is zero within statistical error. These results imply that the influence of field on *the SAR diminishes with increasing temperature.*

In order to determine an upper limit on the change of magnetization across the $\text{LaAlO}_3/\text{SrTiO}_3$ superlattices, we established a relation between the SAR and magnetization in absolute units. The SAR for our samples depends linearly on the change of magnetization across the $\text{LaAlO}_3/\text{SrTiO}_3$ interface. This relationship can be used to calibrate the right hand axes of Figures 3 and 4. If the magnetizations are parallel to the applied field a negative SAR implies that the magnetization in SrTiO_3 is greater than that of LaAlO_3 . For the Sample Twente1 at 11 T and 1.7 K, the SAR is about -0.005 which implies that the SrTiO_3 magnetization is $\sim 2 \text{ emu/cm}^3$, if the magnetization of LaAlO_3 is assumed to be zero. As a consequence, the thickness-weighted average magnetizations of the SrTiO_3 and LaAlO_3 layers, are below the upper limit set by the absence of spin asymmetry at the critical edge of the sample.

Alternatively, if the magnetization is opposite to the applied field, i.e., diamagnetic, a negative SAR implies that the magnetization resides in the LaAlO_3 layer. Our measurements cannot distinguish between induced paramagnetism in SrTiO_3 , or induced diamagnetism in LaAlO_3 .

Overall the SAR of the superlattice reflection in combination with measurements near the critical edge imply that: the magnetization in the LaAlO_3 layer is $\sim 2 \text{ emu/cm}^3$ less than that of the SrTiO_3 layer (or some part thereof), the magnetization of one of these layers is near zero, and the variation of magnetization with depth has the period of the superlattice. If attributed to

Ti, the upper limit for the magnetic moment of 2 emu/cm^3 would correspond to 0.7% of Ti^{3+} per unit cell. This value is of the same order as the few percent of Ti $3d_{xy}$ electrons reported by x-ray spectroscopy.^{17,34} The magnetic scattering centers inferred by Brinkman et al.⁵ may originate from interface Ti^{3+} ions.

The magnetization in $\text{LaAlO}_3/\text{SrTiO}_3$ in our samples is unquestionably small and is not consistent with the large magnetic moments that SQUID (ours or those of Ref. [19]) and torque magnetometry²⁰ attribute to the interface. This discrepancy can either be explained by different growth conditions (magnetotransport effects are most easily observed in samples grown under high O pressure^{5,19} such as used by us), by different interface reconstruction at multilayers compared to bilayers, by bulk contributions to the magnetism, or by use of bulk magnetometry techniques that are prone to artifacts.^{22,23}

In conclusion, we established an upper limit of 2 emu/cm^3 for the change of magnetization across the $\text{LaAlO}_3/\text{SrTiO}_3$ interfaces in superlattices at 11 T and 1.7 K. The upper limit was obtained from measurements of differences between the integrated superlattice Bragg intensities for neutron beam polarization parallel and opposite to the field applied. No significant spin difference was measured near the critical edge of the $\text{LaAlO}_3/\text{SrTiO}_3$ superlattice. Thus, the magnetization *averaged over the entire superlattice* is likely to be less than the upper limit of $\sim 1 \text{ emu/cm}^3$ inferred from measurement of the MgO control, and certainly less for fields less than 11 T or temperatures greater than 1.7 K. These results are inconsistent with magnetization of the order of tens of emu/cm^3 for free electron spin densities

of 10^{21} cm^{-3} aligned by an 11-T field. Some theories of conductivity predict electron spin densities of this magnitude at or near the interface between LaAlO_3 and SrTiO_3 .

Acknowledgements

This work was supported by the Office of Basic Energy Science, U.S. Department of Energy, BES-DMS funded by the Department of Energy's Office of Basic Energy Science. Los Alamos National Laboratory is operated by Los Alamos National Security LLC under DOE Contract DE-AC52-06NA25396. Work at UCM is supported by Consolider Ingenio CSD2009-00013 (IMAGINE), CAM S2009-MAT 1756 (PHAMA) and work at Twente is supported by the Foundation for Fundamental Research on Matter (FOM).

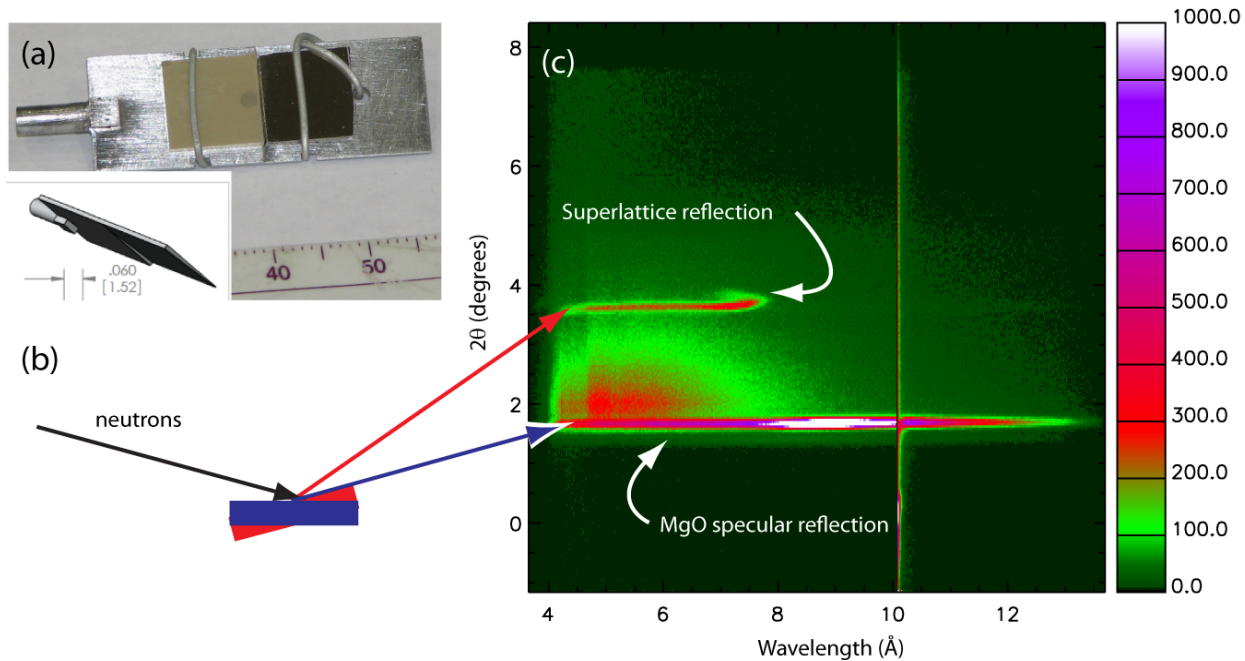


Figure 1 (a) Device used to simultaneously hold the control and LaAlO₃/ SrTiO₃ samples during the PNR experiment. (b) Schematic showing reflection of the neutron beam by the control (blue) and LaAlO₃/ SrTiO₃ sample (red). (c) Neutron intensity image for one beam polarization.

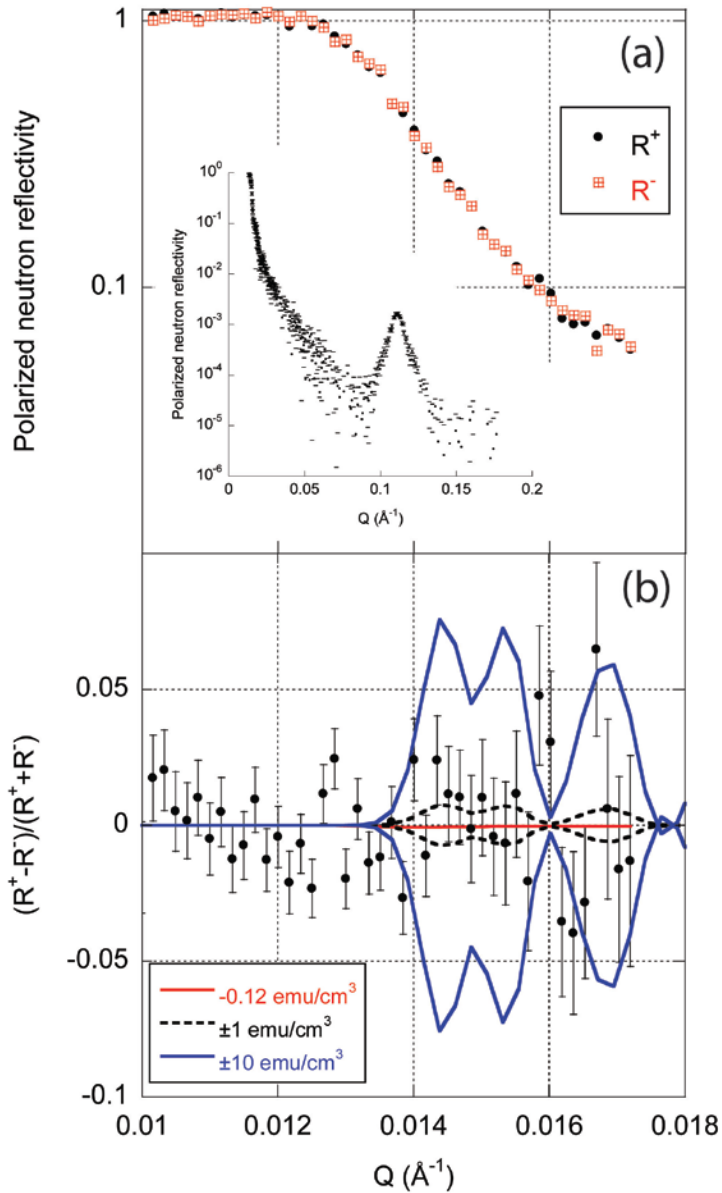


Figure 2 (a) Polarized neutron reflectivity from Twente1 near the critical edge and (inset) R^+ from Madrid1 over a broader range of Q showing the superlattice reflection at $Q = 0.12 \text{ \AA}^{-1}$. (b) The neutron spin asymmetry of Sample Twente1 near the critical edge. (1-sigma errors) Curves correspond to the influence on the spin asymmetry of magnetization uniformly distributed in the superlattice.

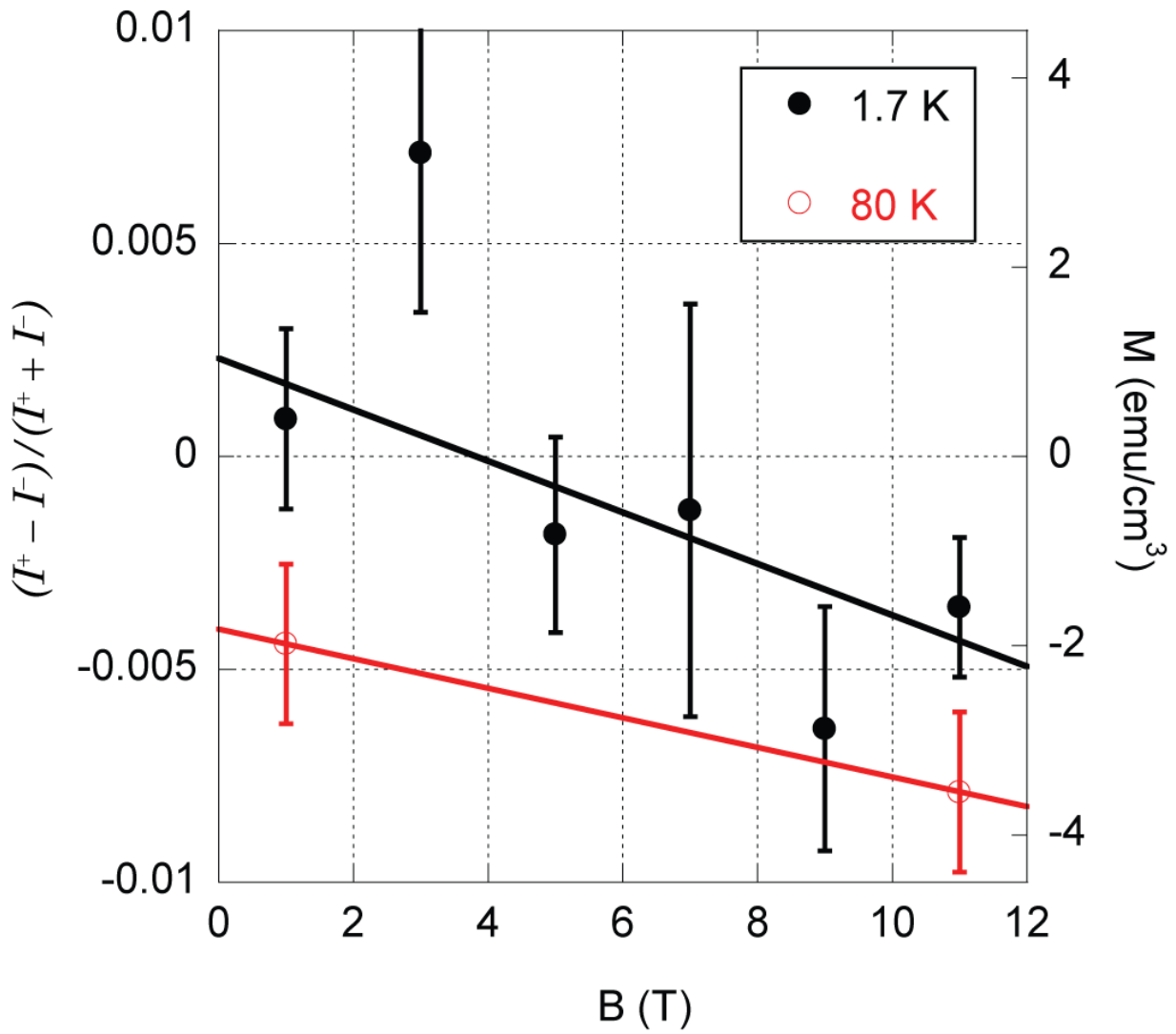


Figure 3 Ratio of the difference over the sum of the integrated intensities, SAR, of the spin dependent superlattice reflections for Twente1 as functions of field and temperature. (1-sigma errors)

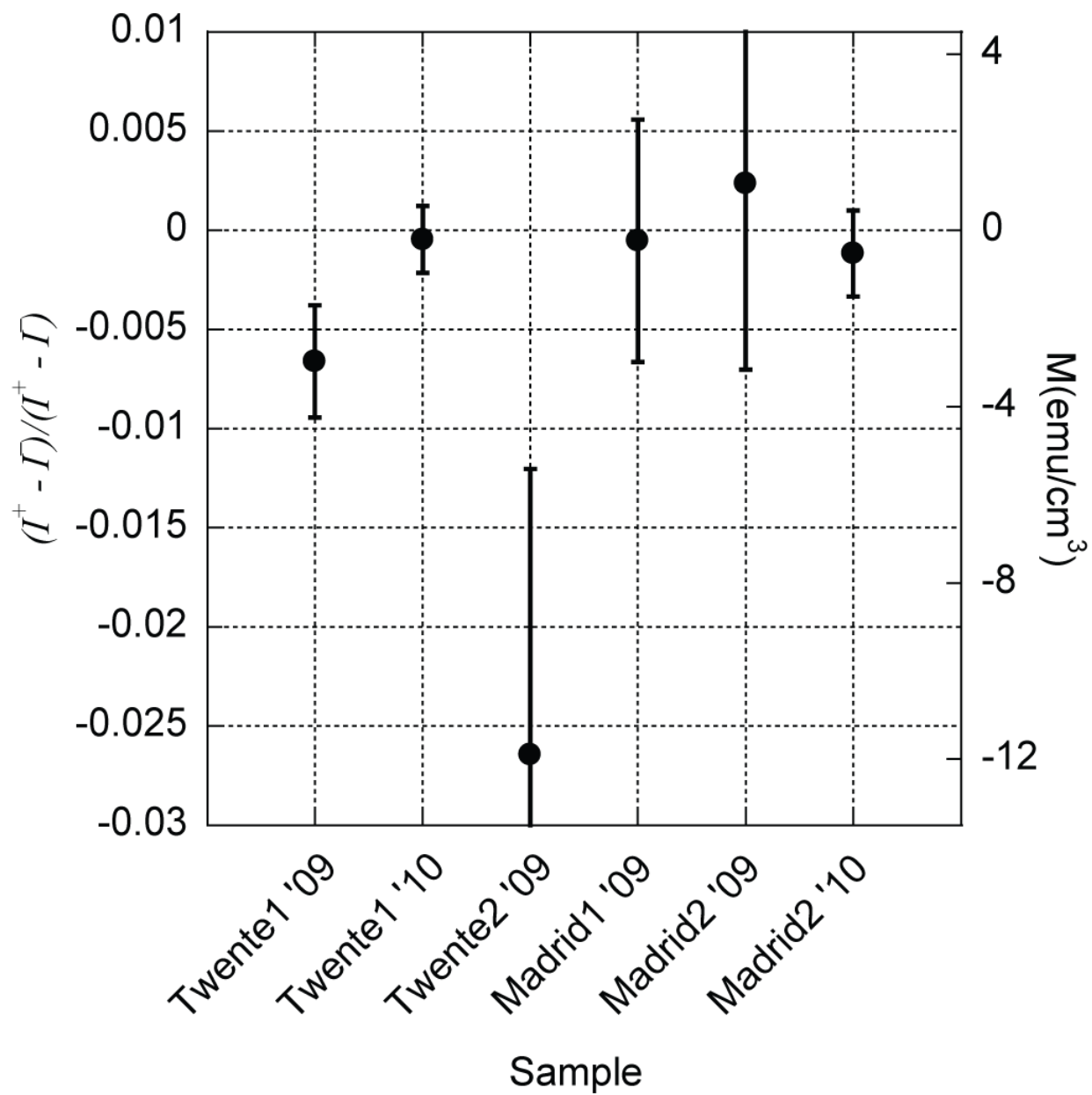


Figure 4 Ratio of the difference over the sum of the integrated intensities, SAR, of the spin dependent superlattice reflections for different samples at 11 T and 1.7 K. (1-sigma errors)

-
- ¹ A. Ohtomo and H.Y. Hwang, *Nature* **427**, 423 (2004).
- ² S. Thiel, G. Hammerl, A Schmehl, C.W. Schneider and J. Mannhart, *Science* **313**, 1942 (2006).
- ³ N. Reyren et al., *Science* **317**, 1196 (2007).
- ⁴ S. Gariglio et al., *J. Phys.: Condens. Matter* **21** 164213 (2009).
- ⁵ A. Brinkman et al. *Nature Materials* **6**, 493 (2007).
- ⁶ D.A. Dikin et al., *Phys. Rev. Lett.* **107**, 056802 (2011).
- ⁷ J.F. Schooley, W.R. Hosler and M.L. Cohen, *Phys. Rev. Lett.* **12**, 474 (1964).
- ⁸ N. Nakagawa et al. *Nature Materials* **5**, 204 (2006).
- ⁹ For a review see, J.N. Eckstein, *Nature* **6**, 473 (2007).
- ¹⁰ K. Yoshimatsu, R. Yasuhara, H. Kumigashira, M. Oshima, *Phys. Rev. Lett.*, **101** 026802 (2008).
- ¹¹ S.A. Chambers, *Phys. Rev. Lett.* **102**, 199703 (2009).
- ¹² K. Yoshimatsu, R. Yasuhara, H. Kumigashira, M. Oshima, *Phys. Rev. Lett.* **102**, 199704 (2009).
- ¹³ A. Kalabukhov et al., *Phys. Rev. B*, **75**, 121404(R) (2007).
- ¹⁴ P.R. Willmott et al. *Phys. Rev. Lett.*, **99** 155502 (2007).
- ¹⁵ A.S. Kalabukhov et al., *Phys. Rev. Lett.* **103**, 146101 (2009).
- ¹⁶ A. Kalabukhov et al., *Euro. Phys. Lett.* **93**, 37001 (2011).
- ¹⁷ M. Salluzzo et al., *Phys. Rev. Lett.* **102**, 166804 (2009).
- ¹⁸ M. Ben Shalom *et al.*, *Phys. Rev. B* **80**, 140403 (2009)
- ¹⁹ Ariando, X. Wang, G. Baskaran, Z.Q. Liu, J. Huijben, J.B. Yi, A. Annadi, A. Roy Barman, A. Rusydi, S. Dhar, Y.P. Feng, J. Ding, H. Hilgenkamp, and T. Venkatesan, *Nat. Comm.* **2**, 188 (2011).

-
- ²⁰ L. Li, C. Richter, J. Mannhart, R.C. Ashoori, arXiv:1105.0235v1 [cond-mat.mtrl-sci] 2 May 2011.
- ²¹ B.J. Kirby, M.R. Fitzsimmons, J.A. Borchers, Z. Ge, X. Liu and J.K. Furdyna, IEEE Trans. on Magnetism, **43**, 3016 (2007)
- ²² J.M.D. Coey and S.A. Chambers, Mater. Res. Bull. **33**, 1503 (2008).
- ²³ M.A. Garcia, E. Fernandez Pinei, J. De la Venta, A. Quesada, V. Bouzas, J.F. Fernández, J.J. Romero, M.S. Martin González and J.L. Costa-Krämer, J. Appl. Phys. **105**, 013825 (2009).
- ²⁴ K. Jannicak, J.P. Velez and E.Y. Tsymbal, J. of Appl. Phys. **103**, 07B508-1 (2008).
- ²⁵ N. Pavlenko, t. Kopp, E.Y. Tsymbal, G.A. Sawatzky, and J. Mannhart, cond-mat\105.1163.
- ²⁶ K. Micheali, A.C. Potter, and P.A. Lee, cond-mat\1107.4352.
- ²⁷ G.P. Felcher *et al.*, Rev. Sci. Instrum. **58**, 609 (1987).
- ²⁸ C.F. Majkrzak, Physica B **221**, 342 (1996).
- ²⁹ M. R. Fitzsimmons and C. Majkrzak, *Modern Techniques for Characterizing Magnetic Materials* (Springer, New York, 2005), Chap. 3, pp. 107–155.
- ³⁰ M.R. Fitzsimmons et al. Phys. Rev. B **76**, 245301 (2007).
- ³¹ In the limit polarization P goes to 1, the true spin difference is related to the observed spin difference by the factor $\frac{1}{P}$. $P > 0.93$ for our experiment.
- ³² L. G. Parratt, Phys. Rev. **95**, 359 (1954).
- ³³ The integration was performed over a region corresponding to two times the root mean square (rms) width of the peak from its center.
- ³⁴ M. Sing et al., Phys. Rev. Lett. **102**, 176805 (2009)